

Catalytic performance of commercial Zeolites Y as catalyst for ethylene production from ethanol dehydration

Jiah Chee Soh^{a,b}, Soo Ling Chong^{a,b}, Sim Yee Chin^a, and Chin Kui Cheng^{a,b,*}

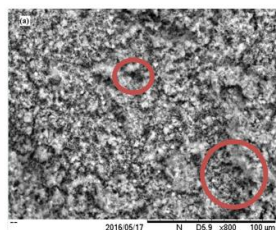
^aFaculty of Chemical and Natural Resources Engineering, Universiti Malaysia Pahang, Malaysia, ^bCentre of Excellence for Advanced Research in Fluid Flow, Universiti Malaysia Pahang, Malaysia, *Corresponding Author: chinkui@ump.edu.my

Article history :

Received 11 October 2016

Accepted 3 November 2016

GRAPHICAL ABSTRACT



SEM images of (a) fresh H-Y (80) 80:1

ABSTRACT

Catalytic dehydration of ethanol into ethylene was studied over commercial zeolites Y with different Si:Al ratios, viz. 5.1:1, 12:1, 30:1, 60:1 and 80:1 and at temperatures that ranged 673 K to 773 K. The physicochemical properties of fresh and spent catalyst of zeolite Y Si:Al 80:1 (best performing catalyst) were investigated using N₂-physisorption, TGA, SEM-EDX, NH₃-TPD, FTIR and XRD. Results showed that fresh zeolites Y with higher Si:Al ratios exhibit better catalytic performance in terms of higher ethanol conversion and higher selectivity to ethylene. Indeed, zeolites Y with Si:Al ratio 5.1:1 and 12:1 demonstrated low catalytic activity with ethanol conversion of 34% and 2%, respectively. However, ethylene selectivity of NH₃-Y (5) was 84%, which was considerably higher than NH₃-Y (12) which was > 26%, indicated that this catalyst was not promoting the formation of other hydrocarbons i.e. methane and ethane. Albeit all of the catalysts, namely H-Y (30), H-Y (60) and H-Y (80) that showed favourable performance in ethanol dehydration (ethanol conversion of 68% and 63%, respectively), the H-Y (80) has yielded almost total selectivity to ethylene and highest conversion of 73.0% among them

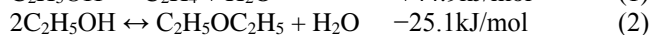
Keywords: Ethanol dehydration; Ethylene; Zeolite Y

© 2017 Dept. of Chemistry, UTM. All rights reserved

| eISSN 0128-2581 |

1. INTRODUCTION

Ethylene is an essential precursor or intermediate in the chemical industry. It serves as the monomer for the synthesis of polyethylene, a material that is widely employed for the production of films for packaging, via polymerization. It is mostly used as the precursor to synthesize Low Density Polyethylene (LDPE) and High Density Polyethylene (HDPE). The demand of polyethylene in the industry outstrips other polymers such as polypropylene and polyvinyl chloride [1]. Commercial production of ethylene is via thermal steam cracking of petroleum hydrocarbon feedstocks such as naphtha from the crude distillation column [2]. Besides steam cracking, other techniques such as Fischer-Tropsch [3], oxidation coupling of methane [4] and catalytic dehydration of ethanol [5–7] have proved to successfully synthesize ethylene in significant amount. There are two competitive pathways during catalytic dehydration of ethanol, viz. the intramolecular dehydration of ethanol to ethylene and, intermolecular dehydration of ethanol to diethyl ether. The reactions can occur in parallel during catalytic dehydration of ethanol:



The main reaction (1) and the side reaction (2) are endothermic and exothermic respectively. Consequently high temperature (300 °C – 500 °C) is more favourable to produce ethylene while low reaction (200 °C – 300 °C) temperature prefers the formation of diethyl ether [8,9].

The dehydration of ethanol to give ethylene is mostly catalyzed over alumina as the catalyst, due to its high distribution of Lewis acidic Al³⁺ sites that act as the active site for ethanol to convert into ethylene. In fact, alumina is the most widely reported catalyst in ethanol dehydration since 1950s. As reported by [10], conversion of ethanol was higher over pure Al₂O₃, with total ethanol conversion and >99% selectivity to ethylene. It is believed that ethanol adsorbs dissociatively on Lewis acid sites. Alumina is commonly doped or promoted with different chemicals to increase the ethanol conversion and enhance the stability for longevity study. A study of ethanol dehydration over Na₂O-doped Mn₂O₃/Al₂O₃ was found to increase in catalytic activities, whereby a significant increase in the conversion percentage of ethanol at 573 K from 22% to 92% [11]. The pyridine chemisorption showed that surface acidity of Na₂O doped alumina was greatly increased when the Na₂O was increased.

Metal oxides have also garnered substantial attentions as catalysts to synthesize olefins due to the basicity and acidity characteristics. A work carried out by Phung and co-workers [12] showed that, both ZrO₂ and TiO₂ can achieve high yields of ethylene (>87%), and titania was observed to

be more active than zirconia in converting ethanol due to the existence of Lewis acid sites as proved in the pyridine adsorption analysis. Besides that, iron oxides (Fe_2O_3) and manganese oxide (Mn_2O_3) also showed increasing ethanol conversion with reaction temperature. Both Fe_2O_3 and Mn_2O_3 have good catalytic activity where the ethanol conversion increased from 42.55% to 96.96% and 38.3% to 90.10%, respectively, at temperature between 473 and 773 K [13].

Zeolites are crystalline solid comprise of silicon, aluminium and oxygen that arranged in a framework with cavities and channels. Zhan and co-workers [7] have modified H-ZSM-5 with phosphorus and lanthanum. Specifically, over a 0.5%La-2%PH-ZSM-5 catalyst, a total ethanol conversion and 99% for ethylene selectivity was achieved. Besides that, the lanthanum-phosphorus modified H-ZSM-5 showed superior stability by reducing coke deposition, as showed by the ethanol conversion and selectivity of 97.4% and 96.4%, respectively, after 72 h. The selectivity of post treated H-ZSM-5 with desilication was highest among the tested catalysts which proved that acidity plays an important role in catalytic activities and desilication can effectively increase the acidic sites [14].

Zeolites Y are those with Si:Al ratio of more than 2.2 [15]. The crystals of zeolite Y consist of frameworks with SiO_4 and AlO_4 tetrahedrons crosslinked by sharing oxygen atoms, with chemical formula of $0.9 \pm 0.2\text{Na}_2\text{O}:\text{Al}_2\text{O}_3:w\text{SiO}_2 \cdot x\text{H}_2\text{O}$, wherein w is a value greater than 3 up to about 6 and x may be a value up to about 9 [16]. Previous research on zeolite Y with Si:Al ratio 5.1:1 showed that the ethanol conversion using this catalyst was relatively low, 1.7% at 373 K compared to other zeolites (H-FER and H-MFI), due to less number of weak and strong Lewis acid sites [17]. Nonetheless, there is no systematic study that reports on effects of zeolite Y with various Si:Al ratios on the catalytic performance. Hence, the effects of Si:Al ratio in zeolites Y and reaction temperature have been investigated in current work. The fresh and spent catalysts were characterized by several techniques including N_2 -physisorption, TGA, NH_3 -TPD, SEM-EDX, FTIR, and XRD.

2. EXPERIMENTAL

2.1 Materials

The commercial lower range zeolites Y (Si:Al = 5.1:1 and 12:1) catalysts were purchased from Alfa Aesar, United States, while higher range zeolites Y (Si:Al = 30:1, 60:1 and 80:1) catalysts were purchased from Zeolyst, United States. Absolute ethanol was purchased from Merck, United States. All the zeolites Y catalysts were used as-received.

2.2 Catalysts Characterization

N_2 physisorption was carried by using a Thermo Scientific Surfer employing mesopores method with approximately 0.3 g of catalyst for each analysis. The sample

was heated to 573 K in a heated built-in sample pouch and maintained at that temperature for overnight to remove moisture and volatile impurities. Subsequently, the sample was transferred to analyzer for N_2 physisorption at 77 K. The total surface area of the spent catalyst was calculated according to the Brunauer-Emmett-Teller (BET) isotherm method while the pore volume was estimated based on Barrett-Joyner-Halenda (BJH) method.

Ammonia temperature-programmed desorption (NH_3 -TPD) was carried out in a Thermo Finnigan TPDRO 1100. The catalyst was pretreated with N_2 at 423 K for 15 min. The adsorption of NH_3 was carried out at room temperature for 45 min and after saturation was achieved, N_2 was purged in to eliminate the remaining NH_3 gas. Analysis of desorption of NH_3 was done under the flow of He at temperatures ranged 323 to 1273 K, at 10 K min^{-1} .

Thermogravimetric analysis (TGA) was performed using a Hitachi STA7200 with approximately 50 mg of catalyst with heating rate 10 K min^{-1} to bring the temperature from room temperature to 1073 K in the atmosphere of high purity air.

The surface morphology and elemental analysis were studied using scanning electron microscopy with X-ray analysis (SEM-EDX) of a Hitachi TM3030Plus brand with an accelerating voltage of 20 kV.

The Fourier transform infrared spectroscopy (FTIR) of catalysts was carried out in a Thermo Nicolet iS50 over the wavenumber that ranged 4000-400 cm^{-1} to determine the functional groups present in the sample and hence can predict the chemical properties of the catalyst.

The X-ray diffraction (XRD) instrument employed was a Rigaku Miniflex II with $\text{CuK}\alpha$ radiation and Ni filter, operated in the vertical mode on 30 kV and 15 mA. The pattern recorded was ranging from 3° to 80° at a scan rate of 2°min^{-1} .

2.3 Reaction Studies

The ethanol dehydration activity evaluation was carried out in a fixed bed reactor. A stainless cylindrical tube with outer diameter (OD) 9.525 mm (0.375") and length of 410 mm (16.14") was constructed. For each run, 0.3 g of catalyst was sandwiched between pom-pom of quartz wool at the centre of the tube and the reaction temperature was detected and accurately controlled by a 1/16" K-type thermocouple placed at the centre of furnace wall. Ethanol partial pressure was set at 33 kPa and the effects of reaction temperature (673K, 723 K and 773 K) were manipulated to study the conversion of ethanol and yield of ethylene. The Alicat MC Series electronic mass flow controller was used to regulate the flow (hence the partial pressure) of diluent gas, N_2 , while Lab Alliance Series 1 HPLC pump was used to regulate the partial pressure or liquid flow rates of ethanol at the inlet. The gaseous products were collected and identified using Shimadzu GC-2011 furnished with a thermal conductivity detector for detecting C_2H_4 and other hydrocarbons. Rtx[®]-1, Rt[®]-Q-BOND and RT[®]-MSIEVE-5A

were used as the columns and Helium was used as the carrier gas at a flow rate 20 ml min⁻¹ STP, and the column and detector temperatures were set at 353 K and 473 K, respectively. The ethanol conversion ($X_{C_2H_5OH}$) and selectivity to ethylene ($S_{C_2H_4}$) were calculated as shown in the formula:

$$X_{C_2H_5OH}(\%) = \frac{2 \times F_{C_2H_4} + \sum_{i=1-6} i \times F_{C_i}}{2 \times F_{C_2H_5OH}} \times 100\% \quad (3)$$

$$S_{C_2H_4}(\%) = \frac{F_{C_2H_4}}{F_T} \times 100\% \quad (4)$$

where $F_{C_2H_4}$, $F_{C_2H_5OH}$ and $F_T = \sum_{i=1-6} i \times F_{C_i}$ represent the flow rate of components.

3. RESULTS AND DISCUSSION

3.1 Catalysts

Table 1 listed some data of the zeolites Y catalysts used in this study. The data is made available by the manufacturers of the commercial catalysts.

Table 1 Textural properties of zeolites Y.

Notation	Commercial name	Manufacturer	Preparation	SiO ₂ /Al ₂ O ₃ mol ratio	Surface area (m ² g ⁻¹)*	Na (%)*
NH ₃ -Y (5)	-	Alfa Aesar	As received	5.1	925	-
NH ₃ -Y (12)	-	Alfa Aesar	As received	12	730	-
H-Y (30)	CBV 720	Zeolyst	As received	30	780	0.03
H-Y (60)	CBV 760	Zeolyst	As received	60	720	0.03
H-Y (80)	CBV 780	Zeolyst	As received	80	780	0.03

* Data from manufacturers.

3.2 Characterization of fresh and spent H-Y (80)

As reported in Section 3.3, zeolite Y with Si:Al 80:1 showed the best catalytic performance in ethanol dehydration over the investigated temperature of 673 to 773 K as the highest ethanol conversion of 73.3% was achieved among all the tested catalysts, thus the fresh and spent H-Y (80) at 773 K and 33 kPa (represents highest dehydration temperature and partial pressure, respectively) ethanol dehydration were selected for the study of physicochemical properties whilst at the same time to investigate the coke deposition behavior. A slight decrease in BET surface area and pore volume was observed from N₂ physisorption analysis. In the analysis, the BET specific surface area and pore volume (calculated based on BJH method) of H-Y (80) before reaction were 780 m² g⁻¹ and 0.47 cm³ g⁻¹ respectively. Both values have decreased to 413.0 m² g⁻¹ and 0.31 cm³ g⁻¹, respectively for the spent catalyst. The slight decrease in BET specific surface area and pore volume could attribute to a mild sintering phenomenon. Consequently, it caused the reduction of active surface on the catalyst during the reaction as ethanol dehydration requires elevated temperature.

The NH₃-TPD was used to characterize the acidic properties of H-Y (80). The TPD profile in the temperature range of 30 to 1000 °C is shown in Fig. 1. It can be observed that H-Y (80) has two ammonia desorption peaks, corresponded to different types of acid sites. The two peaks are located at 135 °C and 314 °C, symptomatic of weak and strong acid sites respectively. The amounts of weak and strong acid sites were found to be 4.3 and 8.0 mmol g⁻¹, respectively. This high number of total acid sites gave better catalytic performance, as proven in reaction studies (refers to Section 3.2), and supported by previous study whereby ethanol dehydration is a comprehensive and synergistic effects of weak and strong acid sites, whereby the amount of weak acid sites are particularly helpful in ethanol dehydration [9].

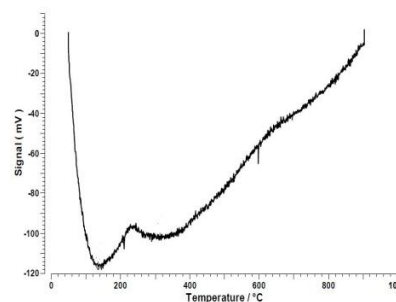


Fig. 1 NH₃-TPD profile of fresh H-Y (80)

TG analysis was also performed on both fresh and spent catalysts and the resulting profiles are shown in Fig. 2. From the figure, it can be observed that the total weight loss for fresh and spent catalysts demonstrate a similar trend, whereby, the total weight loss is about 14wt%. For fresh catalyst, the weight loss can be attributed to the losses of physical and hydration water removal [18]. Significantly, the TG profiles clearly demonstrate the stability of fresh H-Y (80) catalyst up to 900 °C. For the spent catalyst, similar profile was obtained. This infers that there is no carbon deposition or just a very insignificant amount of heavy coke has been deposited on the spent H-Y (80) during the reaction.

SEM-EDX analysis was used to analyze the surface morphology, particle distribution and elemental compositions of fresh and spent H-Y (80). The SEM images including the particle distribution in mapping diagram are shown in Fig. 3 and Fig. 4. The species present in the catalyst is listed in Table 2. From SEM images, it can be observed that the fresh H-Y (80) has a larger pore network (as shown in red circle) compared to the spent H-Y (80). The surface of fresh catalyst also exhibits a rougher and rugged surface. After the catalyst was utilized in the ethanol dehydration, the surface morphology remains unchanged compared to the fresh catalyst. As confirmed in the mapping diagram of Fig. 4(b), carbon (red color) was hardly observed over the surface of spent H-Y (80), and silicon (blue color) was observed to be slightly decreased in the distribution over the surface of spent catalyst. In addition, from EDX analysis, the atomic percentage of spent H-Y (80) also confirmed the presence of

carbon deposited on the catalyst albeit in a negligible amount. The carbon was only 2.11% in spent H-Y (80) and both atomic percentage of aluminium and silicon reduced slightly from 0.93% to 0.87% and 27.83% to 25.68%, respectively, in fresh and spent H-Y (80). The SEM-EDX analysis once again showed that the amount of carbon deposited on spent H-Y (80) was negligible due to the very low atomic percentage as confirmed in the EDX analysis.

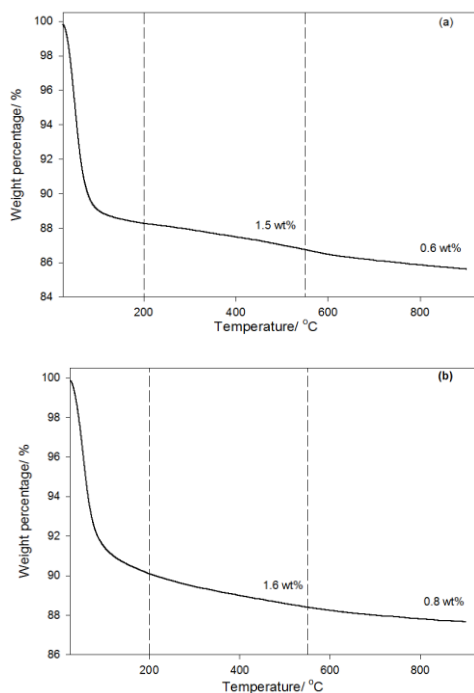


Fig. 2 TG profiles of (a) fresh and (b) spent H-Y (80)

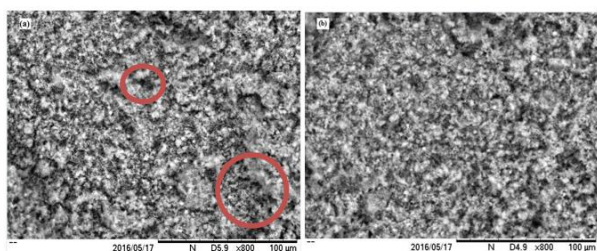


Fig. 3 SEM images of (a) fresh H-Y (80) 80:1 and (b) Spent H-Y (80) 80:1 at magnification of 800 \times .

FTIR spectra of fresh and spent H-Y (80) are shown in Fig. 5 and the vibration frequencies of different species that had been assigned is summarized in Table 3. As shown in Table 3, the vibration frequencies are almost similar to previous reports [19–22]. It can be observed that the spectra for both fresh and spent zeolites consisted of one broad band and several sharp bands at 1048-1056, 830-834 and 453-454 cm^{-1} symptomatic of asymmetric vibrations of Si-O-Si and Si-O-Al, protonated morpholine stretch, and SiO_4 respectively. The FTIR spectra have proven that the chemical structures of fresh and spent catalysts are similar and still intact even after the reaction. Once again, carbon

residue was not detected, consistent with the TG profiles and EDX spectrum.

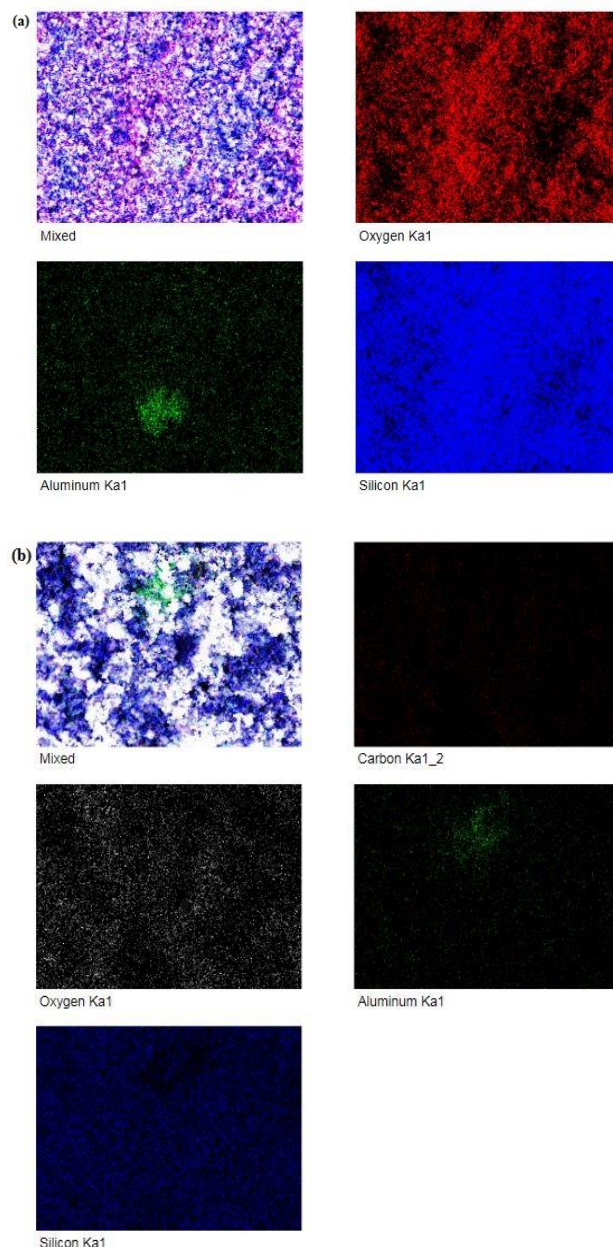


Fig. 4 Particle distributions in (a) fresh H-Y (80) and (b) Spent H-Y (80).

Table 2 EDX analysis on the atomic percentage of fresh and spent H-Y (80).

Element	Atomic percentage /%	
	Fresh	Spent
Oxygen	71.24	71.34
Aluminum	0.93	0.87
Silicon	27.83	25.68
Carbon	-	2.11

XRD patterns of fresh and spent H-Y (80) are shown in Fig. 6. The commercial H-Y (80) before reaction showed a typical Faujasite phase with high crystallinity especially at peaks $2\theta = 6.32^\circ, 10.34^\circ, 12.11^\circ$ and 15.92° [23,24]. The

spent catalyst exhibited similar crystal structure as the parent catalyst, as well as the same crystallite size estimated from the Scherrer equation. The crystallite size of fresh and spent zeolites Y is shown in Table 4. Notably, the crystallite size of spent catalyst showed light increment compared to fresh catalyst. The increment was generally around 5%, an indication of mild sintering.

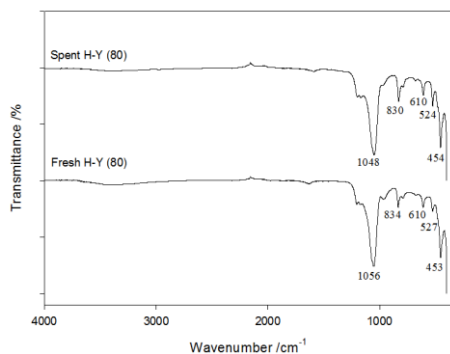


Fig. 5 FTIR spectra of fresh and spent H-Y (80).

Table 3 Vibration frequencies of FTIR bands for fresh and spent H-Y (80).

Samples	IR peaks wavenumber/cm ⁻¹				
	T-O bond	(Si,Al)O ₄	D-6 rings	Protonated morpholine stretch	Asymmetric vibrations of Si-O-Si and Si-O-Al
Fresh	453	527	610	834	1056
Spent	454	524	610	830	1048

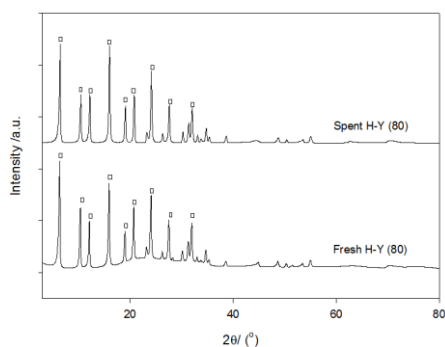


Fig. 6 X-ray diffractograms of fresh and spent H-Y (80) where (□) represents Si₁₉₂O₃₈₄.

Table 4 Average crystalline size of fresh and spent H-Y (80).

2θ	d (Å)	Average crystallite size (nm)	
		Fresh	Spent
6.33	13.96	39.78	41.57
10.34	8.55	36.08	36.72
12.11	7.30	39.19	39.95
15.92	5.562	35.82	37.59

3.3 Reaction Studies

The experimental data for catalytic ethanol dehydration via zeolites Y is shown in Table 5 and the effect of reaction temperature on the catalytic performance of zeolites Y includes the conversion of ethanol and selectivity to ethylene at temperature of 673 to 773 K with time on stream were plotted in Fig. 7 and 8.

The reactivity of zeolites Y was evaluated through ethanol dehydration at various reaction temperatures, from 673 to 773 K, at ethanol partial pressure of 33 kPa. As shown in Table 5, the conversion of ethanol showed either a stable or slight increase trend with increasing reaction temperature for zeolites Y. The distribution of products consisted of mainly ethylene and other carbon compounds such as methane and ethane in a small amount compared to ethylene.

Generally, both the conversion of ethanol and selectivity to ethylene in 60 min reaction showed an increasing trend with increasing reaction temperature. However, from Fig. 7, NH₃-Y (5) showed poor ethanol conversion in dehydration reaction with a decreasing trend in ethanol conversion with increasing temperature, from 32.61% to 26.58%. While NH₃-Y (12) demonstrated the least ethanol conversion among all zeolites Y, which was 2.04% at 673 K and increased to 10.53% in 773 K. In this case, the carrier charge, NH₃⁺ did not affect the catalytic performance during ethanol dehydration. This is because under high reaction temperature or calcination of ammonium types zeolites Y would lead to conversion of NH₃-Y to hydrogen-form zeolite H-Y [24]. Eventually, both NH₃-Y (5) and NH₃-Y (12) were converted into hydrogen form of zeolites Y. Hence, the poor performance of NH₃-Y (12) catalyst (the lowest catalytic performance) was mainly due to the low Si:Al ratio which was 12:1 and low surface area, 730 m² g⁻¹ compared to other tested zeolites Y. H-Y (30), H-Y (60) and H-Y (80) showed a similar trend with a stable and increasing ethanol conversion when the reaction temperature increased from 673 to 773 K. The highest ethanol conversion for these three catalysts was achieved at 773 K, which were 67.09%, 59.71% and 73.33% respectively. From the experimental data, it can be observed that H-Y (80) gives the best ethanol conversion even at low temperature of 673 K. This may attribute to its high surface area and large amount of weak and strong acid sites, which is suitable for catalytic ethanol dehydration.

On the other hand, the selectivity to ethylene in ethanol dehydration over zeolites Y showed a stable trend for various reaction temperatures. However, NH₃-Y (12) displayed the lowest ethylene selectivity compared to other zeolites Y. This catalyst experienced a drastic drop in selectivity when the reaction temperature was 773 K, from 21.9% to 14.3%. The result showed that NH₃-Y (12) has relatively poor catalytic performance in ethanol dehydration due to low ethanol conversion and ethylene selectivity. Another catalyst that also experienced huge decrease in ethylene selectivity was NH₃-Y (5). The highest selectivity was 83.5% at 673 K, but dropped to only 18.4% at 773 K. This indicated that zeolites Y with NH₃⁺ carrier ion studied in this work have lower Si:Al ratio and might not be suitable for ethanol dehydration due to their weak catalytic activities. H-Y (30), H-Y (60) and H-Y (80) all demonstrated a very stable selectivity towards ethylene in ethanol dehydration. Overall, the selectivity was maintained at more than 85%. H-Y (30) and H-Y (60) both have the highest ethylene selectivity of 96.5% and 89.0%, respectively at 673 K, while

lowest selectivity was achieved at 773 K, which were 88.9% and 79.2% respectively. From the results, it can be summarized that Si:Al ratio in zeolites Y greatly affects the catalytic performance as ethylene formation is more favoured in the surroundings of high silica-like structure. The findings was proved in the work by previous research [25]. Thus, H-Y (80) with highest silica content (Si:Al ratio 80:1) displayed the best catalytic performance. Among all the tested zeolites Y, H-Y (80) has the best catalytic performance in the sense of highest ethylene selectivity from 673 to 773 K. The selectivity was well maintained for 60 min

reaction over 98%. Hence, the catalytic performance of zeolites Y in terms of both conversion of ethanol and selectivity to ethylene increase in order of Si:Al ratio 12:1 < 5.1:1 < 60:1 < 30:1 < 80:1.

Table 5 Conversion of ethanol over zeolites Y at various reaction temperatures.

Reaction temperature /K	Ethanol Conversion %				
	NH ₃ -Y (5)	NH ₃ -Y (12)	H-Y (30)	H-Y (60)	H-Y (80)
673	32.6	2.0	67.7	55.6	70.6
723	31.7	2.9	68.3	62.6	72.7
773	26.6	10.5	67.1	59.7	73.3

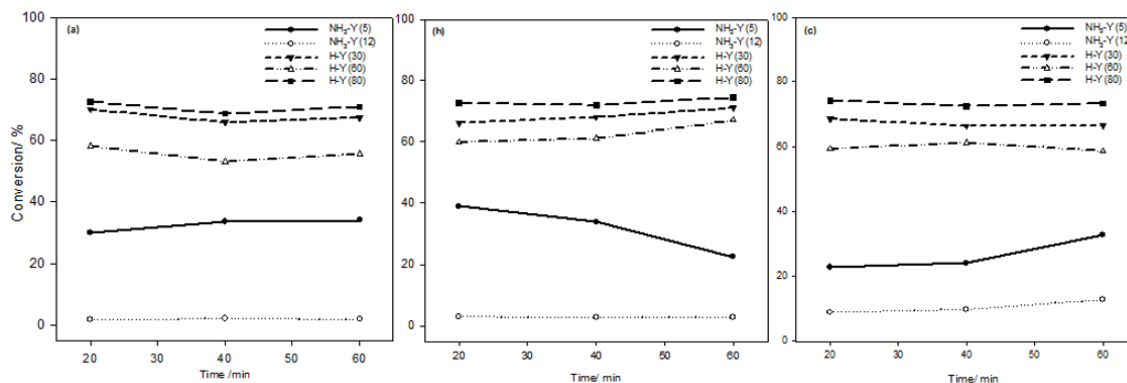


Fig. 7 Conversion of ethanol for zeolites Y at (a) 673 K, (b) 723 K and (c) 773 K. (Reaction condition: WHSV 3×10^4 ml/(g⁻¹ h⁻¹), ethanol partial pressure 33 kPa).

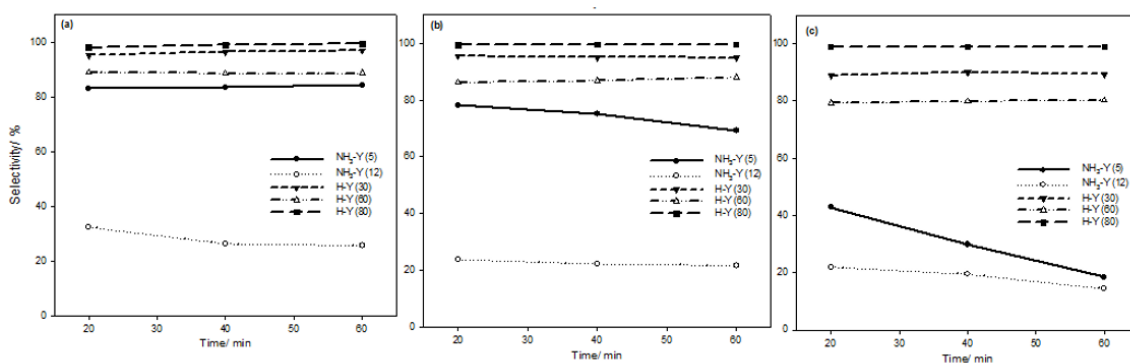


Fig. 8 Selectivity of ethylene for zeolites Y at (a) 673 K, (b) 723 K and (c) 773 K. (Reaction condition: WHSV 3×10^4 ml/(g⁻¹ h⁻¹), ethanol partial pressure 33 kPa).

4. CONCLUSION

The Si:Al ratio in zeolites Y played a significant role in determining the catalytic performance in ethanol dehydration to synthesis ethylene. Zeolite Y with higher Si:Al i.e. H-Y (80) may exhibit higher number of weak and moderate strong acid sites as revealed in the NH₃-TPD analysis, which considerably affects the production of ethylene, causing a higher selectivity to ethylene and better ethanol conversion. Besides, H-Y (80) also proved to exhibit stable catalytic performance by having almost no carbon deposition and suffered a mild sintering, which fortunately does not affect either conversion or selectivity to ethylene.

Thus, the catalytic performance of zeolites Y increase in the order of Si:Al ratio 12:1 < 5.1:1 < 60:1 < 30:1 < 80:1.

ACKNOWLEDGEMENT

This work is supported by Universiti Malaysia Pahang Short Term Grant RDU160335.

REFERENCES

- [1] M.E. Sagel, Polyethylene Global Overview Today's Presentation Global Overview. (2012).
- [2] A. James, United States Patent, 1 (2003).
- [3] A.Y. Khodakov, W. Chu, P. Fongarland, Chem. Rev. 107 (2007) 1692.

- [4] B. Beck, V. Fleischer, S. Arndt, M.G. Hevia, A. Urakawa, P. Hugo, R. Schomäcker, *Catal. Today*. 228 (2014) 212.
- [5] Q. Sheng, S. Guo, K. Ling, L. Zhao, *Chem. Soc.* 25 (2014) 1365.
- [6] K. Ramesh, L.M. Hui, Y.F. Han, A. Borgna, *Catal. Commun.* 10 (2009) 567.
- [7] N. Zhan, Y. Hu, H. Li, D. Yu, Y. Han, H. Huang, *Catal. Commun.* 11 (2010) 633.
- [8] G. Chen, S. Li, F. Jiao, Q. Yuan, *Catal. Today*. 125 (2007) 111.
- [9] Y. Chen, Y. Wu, L. Tao, B. Dai, M. Yang, Z. Chen, X. Zhu, *J. Ind. Eng. Chem.* 16 (2010) 717.
- [10] T.K. Phung, A. Lagazzo, M.Á. Rivero Crespo, V. Sánchez Escribano, G. Busca, *J. Catal.* 311 (2014) 102.
- [11] M. Doheim, *Mater. Lett.* 55 (2002) 304.
- [12] T.K. Phung, L. Proietti Hernández, G. Busca, *Appl. Catal. A Gen.* 489 (2015) 180.
- [13] T. Zaki, *J Colloid Interf Sci*, 284 (2005) 606.
- [14] H. Xin, X. Li, Y. Fang, X. Yi, W. Hu, Y. Chu, F. Zhang, A. Zheng, H. Zhang, X. Li, *J. Catal.* 312 (2014) 204.
- [15] W. Lutz, *Adv. Mater. Sci. Eng.* 2014 (2014) 1.
- [16] S. Stapler, United States Patent, 1 (2002).
- [17] T.K. Phung, G. Busca, *Appl. Catal. A Gen.* 504 (2015) 151.
- [18] K. Ramesh, C. Jie, Y.F. Han, A. Borgna, *Ind. Eng. Chem. Res.* 49 (2010) 4080.
- [19] S. Ashtekar, S.V. V Chilukuri, D.K. Chakrabarty, *J. Phys. Chem.* 98 (1994) 4878.
- [20] Y. Tao, H. Kanoh, K. Kaneko, *J. Phys. Chem.* 107 (2003) 10974.
- [21] L.-P. Wu, X.-J. Li, Z.-H. Yuan, Y. Chen, *Catal. Commun.* 11 (2009) 67.
- [22] D. Zhang, R. Wang, X. Yang, *Catal. Letters.* 124 (2008) 384.
- [23] B.A. Holmberg, H. Wang, J.M. Norbeck, Y. Yan, *Microporous Mesoporous Mater.* 59 (2003) 13.
- [24] J.J.F. Saceda, K. Rintramee, S. Khabuanchalad, S. Prayoonpokarach, R.L. de Leon, J. Wittayakun, *J. Ind. Eng. Chem.* 18 (2012) 420.
- [25] T.K. Phung, G. Busca, *Catal. Commun.* 68 (2015) 110.